Polaron Spin-Lattice Relaxation Time in π-Conjugated Polymers from Optically Detected Magnetic Resonance

C. G. Yang,[1] E. Ehrenfreund,[1,2] and Z. V. Vardeny[1]

[1]*Department of Physics, University of Utah, Salt Lake City, Utah 84112, USA*
[2]*Department of Physics, Technion-Israel Institute of Technology, Haifa 32000, Israel*

We describe a method for obtaining the polaron spin-lattice relaxation time T_{SL} in π-conjugated polymers by measuring the optically detected magnetic resonance (ODMR) dynamics as a function of microwave power and laser intensity. The peculiar ODMR dynamics is well described by a spin dependent recombination model where both recombination and spin relaxation rates determine together the response dynamics. We apply this method to the spin $1/2$ ODMR in films of pristine 2-methoxy-5-(2'-ethylhexyloxy) phenylene vinylene [MEH-PPV] polymer, as well as MEH-PPV doped with various concentrations of radical impurities. We obtained $T_{SL} \sim 30$ μs in pristine MEH-PPV, but substantially shorter when the magnetic impurities are added.

PACS numbers: 78.55.Kz, 73.61.Ph, 76.70.Hb

Numerous studies have been recently completed for understanding the spin and magnetic field effects in organic semiconductors (OSEC) [1–4]. The surge in organic spin research stems from the premise of long carrier spin relaxation time T_{SL} in these materials due to the weak spin-orbit coupling caused by the light atoms of their building blocks; this property is very attractive for potential applications in Spintronics devices [1]. This proposition was recently supported by several demonstrations of organic spin valves using small molecule and polymer films as spacers between two ferromagnetic electrodes, where a relatively large spin-valve magnetoresistance response was measured [2–4]. Also low field magnetotransport response up to 10% was demonstrated in various organic light emitting diodes [5]. One of the important physical parameters in such organic spintronic devices is T_{SL} that determines the spin randomization rate, and ultimately the spin diffusion length in the OSEC active layer [1,2]. However, at the present time there is no method for determining T_{SL} of excess carriers (polarons) in OSEC. In this Letter we introduce a simple method for obtaining T_{SL} of polarons in OSEC, which is based on the dynamics of the optically detected magnetic resonance (ODMR) response in these materials.

Since ODMR involves the spin sublevels response to double excitation, namely, laser illumination (or carrier injection), and microwave (MW) radiation under spin resonance conditions [6]; then this technique is uniquely sensitive to both excess-carrier recombination rate γ *and* spin-lattice relaxation rate $\gamma_{SL}(= T_{SL}^{-1})$. In principle ODMR may be described as electron spin resonance (ESR) of the optically generated (or electrically injected) excitations. Whereas the initial spin sublevel populations in ground state ESR measurements is determined by the temperature; under resonant MW radiation at saturation the relative sublevel population dynamics is mainly controlled by T_{SL} [7]. In contrast to ESR the sublevel populations in

ODMR continuously evolve due to excess-carrier generation and recombination kinetics, so that their MW modulation frequency (f) response depends on *both* recombination and spin-lattice relaxation rates [8]. This renders the ODMR frequency response peculiar, and thus distinctly different from that of a single excitation, such as in photoinduced absorption (PA) or photoluminescence (PL).

Specifically, we show in this Letter that unlike the usual response dynamics of pump modulated PA(f) and PL(f), the in-phase (I) ODMR(f) component *reverses sign* at a modulation frequency f_0. Importantly we found that f_0 depends on γ, γ_{SL}, and the MW power, P_{MW}, and thus a thorough analysis of the ODMR dynamics response gives the important rates involved. In particular by analyzing the spin $1/2$ ODMR dynamics as a function of P_{MW} and laser intensity (I_L) using a simple spin dependent recombination model, we show that it is possible to obtain both γ and γ_{SL} (and hence also T_{SL}) for polarons in OSEC. We demonstrate our powerful analysis for polarons in pristine films of 2-methoxy-5-(2'-ethylhexyloxy) phenylene vinylene [MEH-PPV], as well as MEH-PPV doped with various concentrations of magnetic nanoparticles and radical impurities. Our technique is not restricted to OSEC, or to spin $1/2$ excitations; in fact we could equally well analyze the ODMR response in inorganic semiconductors, such as amorphous Si:H [9] with similar success.

The spin $1/2$ ODMR (either PADMR or PLDMR) measurements were conducted at various temperatures T using a MEH-PPV film drop casted from a toluene solution that was mounted in a high Q ($\sim 10^3$) MW cavity. The polymer film was excited using an Ar$^+$ laser at 488 nm with intensities from 50 to 1500 mW/cm^2 subjected to spin $1/2$ (i.e., $H = 1070$ Gauss) resonance conditions at MW frequency, $f_{MW} \sim 3$ GHz (S band) [6]. We measured the dynamic changes ΔPL(f) [ΔPA(f)] in PL [PA] caused by the magnetic resonance. Both the in-phase ODMR$_I$ and quadrature ODMR$_Q$ components were measured, where

the phase was set with respect to the MW modulation. In addition, the ODMR was also studied under variable MW power conditions, where P_{MW} was varied from 2.5 to 100 mW.

Figure 1(a) shows the spin 1/2 PLDMR response dynamics for the two ODMR components. A unique and peculiar feature is that $ODMR_I(f)$ *changes sign* at a frequency f_0 of ~30 kHz, before decaying away at higher frequencies. This response is unique to $ODMR_I$; $ODMR_Q$, on the contrary, retains its sign. Figure 1(b) shows that f_0 increases with P_{MW}; it increases more sharply at low P_{MW}

and saturates at high P_{MW}. The P_{MW} dependence of the ODMR maximum value ([ODMR]$_{max}$) at low f obtained from several dynamic responses such as in Fig. 1(b), is summarized in Fig. 2; [ODMR]$_{max}$ shows a typical saturation behavior.

The surprising $ODMR_I$ "zero-crossing" at f_0, and its dependence on P_{MW} can be explained in detail by a spin dependent recombination model for polarons [6,10]. A variation of this model known in the literature as the "distant pair recombination model" [11] has been used previously in inorganic semiconductors [11,12]. In this model, polaron pairs with antiparallel spins (having population n_1 and lifetime τ_1) recombine faster than polaron pairs with parallel spins (having population n_2 and lifetime τ_2), i.e., $\tau_1 < \tau_2$. If the polaron pair spin sublevel populations are formed with equal generation rate G, then at steady state (SS) conditions (i.e., $n_{SS} = G\tau$) without MW radiation (dark, d) "spin polarization" is established; namely $n_{1,d} < n_{2,d}$. The MW radiation induces spin flips, and a new quasiequilibrium state, n_{mw} is established; where the MW induced change $\Delta n = n_{mw} - n_d$ in the polaron density, $n = n_1 + n_2$ is proportional to the ODMR signal [13]. The quantitative $\Delta n(f)$ response can be then obtained from the solution of the following coupled set of two rate equations, written for the experimental conditions $T \gg hf_{MW}/k_B \cong 0.14$ K [12]:

$$dn_i/dt = G - n_i/\tau_i - (n_i - n_j)/2T_{SL} - (n_i - n_j)P,$$
(1)

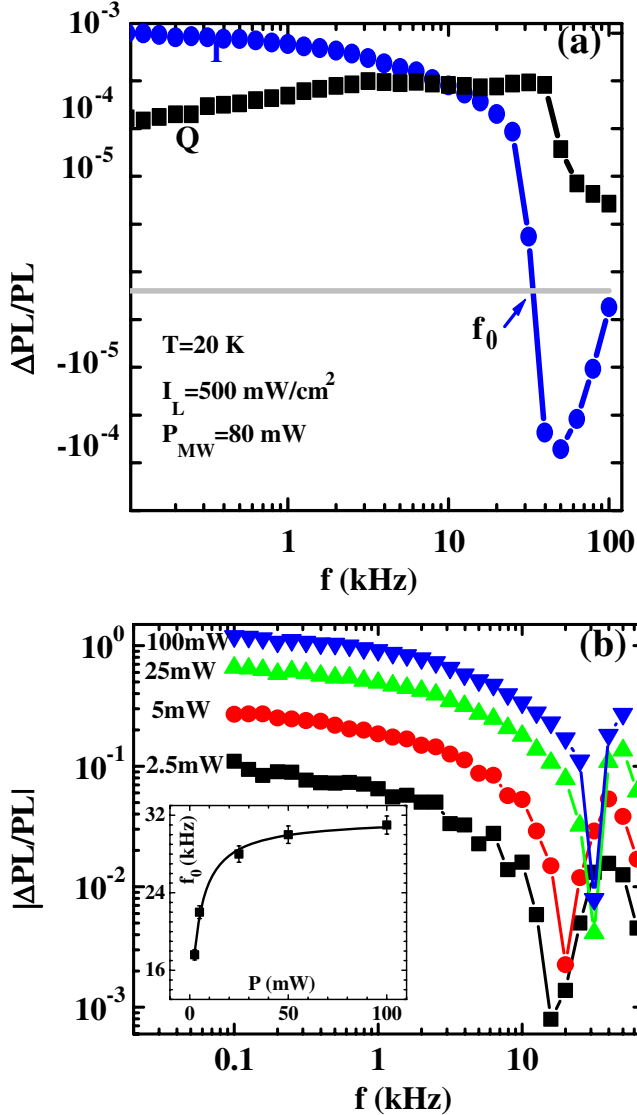where $i \neq j = 1, 2$, and P is the MW induced spin-flip rate

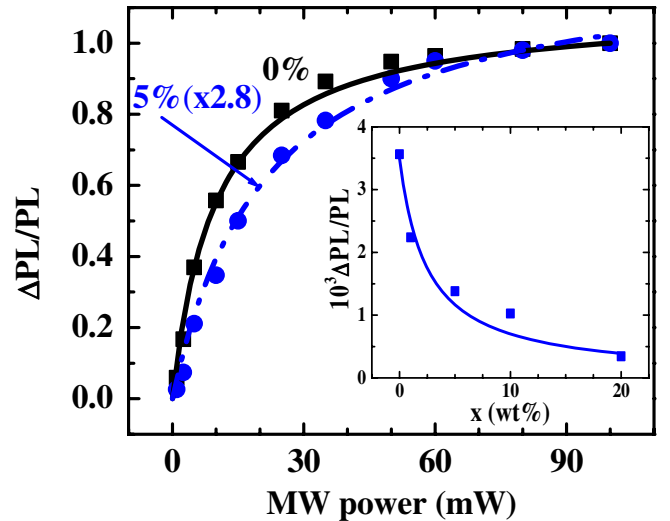FIG. 1 (color online). (a) In-phase (●, blue or dark gray) and quadrature (■, black) spin 1/2 PLDMR vs the MW modulation frequency f in MEH-PPV film; zero crossing occurs at f_0. The positive and negative values are displayed, respectively, on a logarithmic scale above and below the gray horizontal line. (b) Absolute value |PLDMR$_I$| vs f for various P_{MW}, where the dip occurs at f_0. Inset: the zero-crossing frequency f_0 vs P_{MW}.

FIG. 2 (color online). ODMR$_{max}$ vs P_{MW} for pristine (■, black) and doped (●, blue or dark gray) MEH-PPV with $x = 5$ wt % spin 1/2 radicals. The solid lines are fits using Eq. (2) with $\gamma^*_{5\%} = 2.2\gamma^*_{0\%}$, where the $x = 5$ wt % is normalized to the pristine data. Inset: ODMR$_{max}$ vs x measured at saturation conditions. The solid line is a fit using Eq. (2) with $\gamma_{SL}(x) - \gamma_{SL}(0) \propto x$.

that is proportional to the modulated P_{MW}: $P = \alpha P_{MW}$. Equations (1) were solved numerically in response to the modulated MW radiation, yielding the components Δn_I and Δn_Q vs the modulation frequency f; this procedure was repeated at various P's.

A typical spin $1/2$ ODMR(f) response based on the numerical calculation of Eqs. (1) is shown in Fig. 3. There are three important quantitative features of the calculated ODMR response that reproduce the data: (i) Δn_I changes sign at f_0; (ii) Δn_Q does not change sign; and (iii) f_0 increases with P. Δn_I sign reversal at f_0 is unique to ODMR, and does not depend on the model or parameters used [8]; in fact it is a manifestation of the different recombination times τ_i of the two coupled spin sublevels. This peculiar response occurs since under resonant MW radiation the density of one spin sublevel increases by an initial value δn, whereas the other decreases by the same amount. However, $\delta n(t)$ decays faster in sublevel 1 than in sublevel 2. It thus follows that $\Delta n_I(f)$ changes sign at a frequency f_0 that roughly corresponds to the average decay rate of the two sublevels, but is also influenced by T_{SL}.

Solving Eqs. (1) using numerical methods, we thoroughly studied the dependence of $\Delta n(\omega)$ response on the parameters G, P, and T_{SL}, while keeping fixed the recombination rate $\gamma = \frac{1}{2}(\tau_1^{-1} + \tau_2^{-1})$. Since ODMR is closely related to ESR, we looked for a saturation behavior at large P. We found that $\Delta n(\omega \cong 0)$ indeed saturates and may be written approximately as $\Delta n(\omega \cong 0) \propto P/(\gamma^* + P)$, where $\gamma^* = C(\gamma, \gamma_{SL}, \Delta\gamma)$ [14] $\simeq \frac{2}{3}(\gamma + \gamma_{SL})$, where $\Delta\gamma = \frac{1}{2}(\tau_1^{-1} - \tau_2^{-1})$. It is thus apparent that saturation

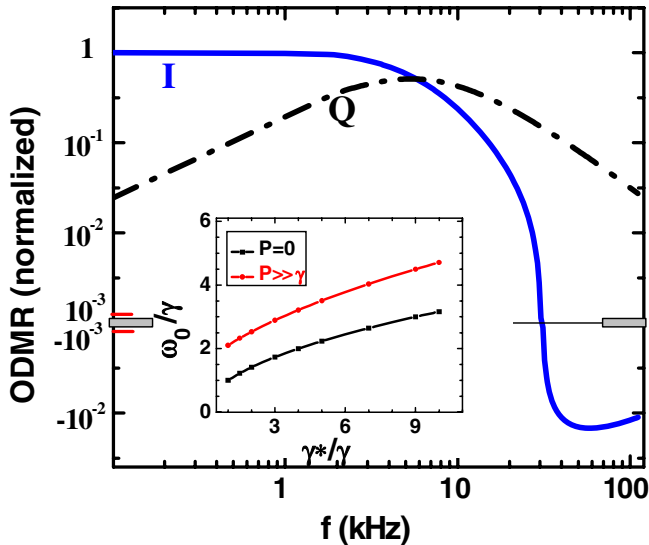FIG. 3 (color online). The ODMR dependence on f calculated using Eq. (1) with $\gamma = 4.4 \times 10^4$ s^{-1} and $\gamma_{SL} = 3.6 \times 10^4$ s^{-1}, with same color (or shading) codes and symbols as in Fig. 1(a). The positive and negative values are displayed, respectively, on a logarithmic scale above and below the gray horizontal line. Inset: f_0 vs γ^*/γ calculated at small and large P_{MW}.

depends on both γ and γ_{SL} (rather than on γ_{SL} alone as in ESR measurements). Next, we checked the low frequency response as a function of γ_{SL} while keeping fixed P at saturation (i.e., $P \gg \gamma^*$); we found that Δn is inversely proportional to γ^*. We may thus approximate the low frequency ODMR response by the relation

$$\Delta n(\omega \cong 0) \propto (G/\gamma^*)P/(\gamma^* + P). \tag{2}$$

This relation is in agreement with an approximate analytical solution of Eqs. (1) at low f [13]. In addition, the dependence of f_0 on P was also obtained numerically for various γ^*/γ values. We found that $\omega_0 \simeq (\gamma\gamma^*)^{1/2}$ for $P \ll \gamma^*$. Also at $P \gg \gamma^* \omega_0$ continuously increases, then saturates at large P, in agreement with the data [Fig. 1(b)].

By fitting the experimental [ODMR]$_{max}$ (Fig. 2), and f_0 [Fig. 1(b) inset] as a function of P_{MW} using Eq. (2) and the f_0 values at low and saturated P's, we deduce the rates γ and γ^*. We thus obtained for polarons in pristine MEH-PPV $\gamma \sim 4.4 \times 10^4$ s^{-1} and $\gamma_{SL} \sim 3.6 \times 10^4$ s^{-1} (i.e., $T_{SL} \sim 30$ μsec) at $I_L = 500$ mW/cm^2. The calculated response (Fig. 3) accurately reproduces the "zero crossing" of $\Delta n_I(f)$ at the measured frequency, whereas $\Delta n_Q(f)$ does not change sign.

In order to further study the ODMR dynamics we introduced magnetic impurities into the MEH-PPV film by mixing the polymer solution with a predetermined impurity dose [15]. Introducing even a small amount of spin $1/2$ radical ions [the free radical used was 2,2,6,6-tetramethyl-piperidine-1-oxyl (TEMPO)], or mixing with ferromagnetic Fe$_3$O$_4$ nanoparticles gives rise to dramatic effects. As shown in Fig. 2 for the radicals: (i) the ODMR signal significantly decreases with the radical concentration x; and (ii) the saturation of the ODMR signal occurs at higher P_{MW} in the mixed polymer-radical films. From the fit to the $x = 5\%$ data using Eq. (2) we found that γ^* increases in doped MEH-PPV by a factor of ~ 2.2 relative to the pristine MEH-PPV. Since the magnetic radicals are not expected to have a strong effect on the recombination rate γ, we conclude that the increase in $\gamma^*(\propto \gamma + \gamma_{SL})$ is due mostly to a decrease in T_{SL} caused by the spin $1/2$ radicals. Using the γ and T_{SL} values of pristine MEH-PPV obtained above, we find for the MEH-PPV/TEMPO film at $x = 5\%$ that T_{SL} shortens by a factor of ~ 4.

In addition, [ODMR]$_{max}$ measured under saturating MW power at $f = 200$ Hz decreases with increasing radical concentration, x (Fig. 2, inset). This can be well explained by Eq. (2): the solid line (Fig. 2, inset) is a fit assuming that γ_{SL} increases linearly with x: $\gamma_{SL}(x) - \gamma_{SL}(0) \propto x$. Such a linear increase may occur via *spin-spin dipolar interaction* between the photogenerated polaron and radical spins, which randomizes their spins.

The variation in the ODMR dynamics with the laser intensity I_L provides additional insights as seen in Fig. 4: (i) f_0 increases with I_L, and (ii) [ODMR]$_{max}$ saturates at higher P_{MW} for higher I_L. From the fit to the ODMR
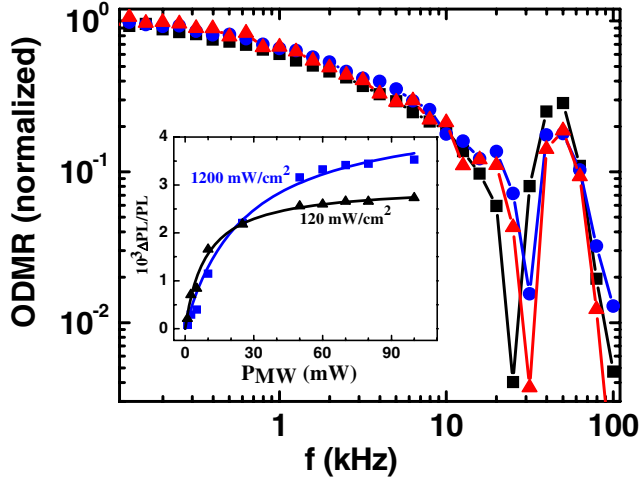
FIG. 4 (color online).   Spin 1/2 PLDMR$_I$ dynamics in pristine MEH-PPV for various laser excitation intensities, I_L at $T = 20$ K and $P_{MW} = 100$ mW. $I_L = 90$ (■, black), 500 (●, blue or dark gray), and 1500 (▲, red or gray) mW/cm^2. Inset: PLDMR$_{max}$ vs P_{MW} measured at $f = 200$ Hz for $I_L = 1200$ (■, blue or dark gray) and 120 mW/cm^2 (▲, black). The solid lines are fits obtained using Eq. (2), with $\gamma^*_{1200} = 2.8\gamma^*_{120}$.

saturation behavior at two I_L using Eq. (2), we obtained $\gamma^*_{1200} = 2.8\gamma^*_{120}$. The increase in γ^* also explains the corresponding increase of f_0 with I_L seen in Fig. 4. γ^* increase with I_L may be explained by an increase in γ_{SL} via spin-spin dipolar interaction, similar to the mixed MEH-PPV/TEMPO discussed above; where the increased density of unpaired spin 1/2 polarons at large I_L plays the role of magnetic impurities. The obtained increase in γ^* may be also explained by an increase in γ caused by nonlinear recombination kinetics, where the magnetically coupled pair dynamics at high I_L is affected by neighboring paired and unpaired polarons. Our results thus indicate that T_{SL} of polaron pairs formed in organic light emitting diodes upon current injection should depend on the injected current density, which is actually equivalent to introducing spin 1/2 magnetic impurities into the active film.

[1] V. Dediu *et al.*, Solid State Commun. **122**, 181 (2002).
[2] Z. H. Xiong, D. Wu, Z. V. Vardeny, and J. Shi, Nature (London) **427**, 821 (2004).
[3] S. Majumdar, R. Laiho, P. Laukkanen, I. J. Väyrynen, H. S. Majumdar, and R. Österbacka, Appl. Phys. Lett. **89**, 122114 (2006).
[4] T. S. Santos, J. S. Lee, P. Migdal, I. C. Lekshmi, B. Satpati, and J. S. Moodera, Phys. Rev. Lett. **98**, 016601 (2007).
[5] Ö. Mermer, G. Veeraraghavan, T. L. Francis, Y. Sheng, D. T. Nguyen, M. Wohlgenannt, A. Köhler, M. K. Al-Suti, and M. S. Khan, Phys. Rev. B **72**, 205202 (2005).
[6] Z. V. Vardeny and X. Wei, in *Handbook of Conducting Polymers* (Marcel Dekker, Inc., New York, 1998), 2nd ed., p. 639.
[7] G. E. Pake, *Paramagnetic Resonance* (Benjamin, Inc., New York, 1962).
[8] C. Boehme and K. Lips, Phys. Rev. B **68**, 245105 (2003).
[9] R. A. Street, D. K. Biegelsen, and J. Zesch, Phys. Rev. B **25**, 4334 (1982).
[10] M. Wohlgenannt, K. Tandon, S. Mazumdar, S. Ramasesha, and Z. V. Vardeny, Nature (London) **409**, 494 (2001).
[11] B. C. Cavenett, Adv. Phys. **30**, 475 (1981).
[12] E. Lifshitz, L. Fradkin, A. Glozman, and L. Langof, Annu. Rev. Phys. Chem. **55**, 509 (2004).
[13] M. Wohlgenannt and Z. V. Vardeny, in *Handbook of Organic Electronics and Photonics*, edited by H. S. Nalwa (American Scientific Publishers, Stevenson Ranch, CA, 2007).
[14] $C(\gamma, \gamma_{SL}, \Delta\gamma) = 1 - (\Delta\gamma)^2[\gamma(\gamma + \gamma_{SL})]^{-1}$.
[15] C. G. Yang, Ph.D. thesis, University of Utah, 2006 (unpublished).